Band structure engineering of graphene by strain: First-principles calculations

Gui Gui, Jin Li, and Jianxin Zhong*

Laboratory for Quantum Engineering and Micro-Nano Energy Technology, Xiangtan University, Xiangtan 411105, Hunan, People's Republic of China

and Department of Physics, Xiangtan University, Hunan 411105, People's Republic of China

(Received 7 November 2007; revised manuscript received 3 June 2008; published 25 August 2008)

We have investigated the electronic structure of graphene under different planar strain distributions using the first-principles pseudopotential plane-wave method and the tight-binding approach. We found that graphene with a symmetrical strain distribution is always a zero band-gap semiconductor and its pseudogap decreases linearly with the strain strength in the elastic regime. However, asymmetrical strain distributions in graphene result in opening of band gaps at the Fermi level. For the graphene with a strain distribution parallel to C-C bonds, its band gap continuously increases to its maximum width of 0.486 eV as the strain increases up to 12.2%. For the graphene with a strain distribution perpendicular to C-C bonds, its band gap continuously increases only to its maximum width of 0.170 eV as the strain increases up to 7.3%. The anisotropic nature of graphene is also reflected by different Poisson ratios under large strains in different directions. We found that the Poisson ratio approaches to a constant of 0.1732 under small strains but decreases differently under large strains along different directions.

DOI: 10.1103/PhysRevB.78.075435 PACS number(s): 73.22.−f, 73.61.Wp, 72.80.Rj

Graphene, a single-layer graphite sheet, is a zero band-gap semiconductor.[1,2] Since obtained successfully in 2004,[1] it has attracted tremendous interests of theoretical and experimental studies. Graphene has unique electronic properties arising from its hexagonal honeycomb lattice structure, which makes electrons in graphene behave as massless relativistic fermions that satisfy the Dirac equation.[3] The quantum Hall effect[4] has been observed in graphene. Studies have also shown that spin-orbital coupling exists in graphene[5–8] and the quantum spin Hall effect may occur at ultralow temperature.[8] These and other unusual electronic properties of graphene make it a promising material for building electronic devices. Nevertheless, absence of band gap in graphene sets limitations on its practical applications. It is of crucial importance to find methods to effectively tune the band gap of graphene for broadening its applications in nanoelectronics and optoelectronics. Recently, much attention was devoted to the study of substrate-induced gap opening in graphene associated with inversion symmetry breaking.[9,10] It has been shown that graphene systems without inversion symmetry breaking possess unique magnetic and optical properties.[10]

We have studied the electronic structure of graphene under different planar strain distributions by the first-principles pseudopotential plane-wave method and the tight-binding (TB) approach. Our results show that strain distributions in graphene significantly modify the band structure of graphene around the Fermi level, resulting in remarkable change of the pseudogap width in the case of symmetrical strain distributions and band-gap opening in the case of asymmetrical strain distributions, which break the inversion symmetry. Our findings indicate that electronic transport properties of graphene can be effectively tuned by applying planar forces to graphene along different directions.

Our calculations were performed using the density-functional theory (DFT) method implemented in the plane-wave basis VASP (Refs. 11 and 12) code. We used the projector augmented wave (PAW) (Refs. 13 and 14) potentials and the generalized gradient approximation (GGA) of Perdew and Wang[15] known as PW91. The total energy was converged to within 1 meV with a kinetic-energy cutoff of 550 eV and a Monkhorst-Pack[16] k-point mesh of $21\times21\times1$ (Γ included). Atoms were fully relaxed using a conjugate gradient (CG) algorithm until the interatomic forces are less than 0.1 eV/nm. In order to eliminate interactions between graphene layers, 2.05 nm of vacuum separation along the c axis was used.

First, we studied the electronic properties of graphene in the absence of strain, and found an in-plane lattice constant of 0.246 69 nm, which is in good agreement with the experiment value 0.2461 nm, and a direct zero band gap between π bands crossing at each corner (K point) of the two-dimensional (2D) hexagonal Brillouin zone[17] [see Fig. 2(a)]. The results confirmed that VASP and the PAW method are reliable and flexible to graphene. Sequentially, the electronic properties of graphene with three types of strain distributions were studied, namely: (i) symmetrical strain distribution (keeping the hexagonal symmetry unchanged) as shown in Fig. 1(a), (ii) asymmetrical distribution perpendicular to C-C bonds as shown in Fig. 1(b), and (iii) asymmetrical strain distribution parallel to C-C bonds as shown in Fig. 1(c).

For the graphene with symmetrical strain distribution, systems with lattice constants from 0.2009 to 0.5099 nm by step of 0.005 nm were investigated. Figure 2(a) shows the band structure, density of states (DOS), and electron localization function (ELF) of the graphene systems with lattice constants of 0.2259, 0.246 69, 0.2709, 0.3209, 0.3759, and 0.4509 nm. From Fig. 2(a), one can see that there is no band-gap opening around the Fermi level for the graphene with any strength of symmetrical tensile or compressive strain. Nevertheless, strain results in remarkable change of the pseudogap width around the Fermi level, as shown in Fig. 2(b). Tensile strain results in decrease in the pseudogap while compressive strain leads to increase in the pseudogap.

The ELFs in Fig. 2(a) show that the size of the high electron localization region between two carbon atoms

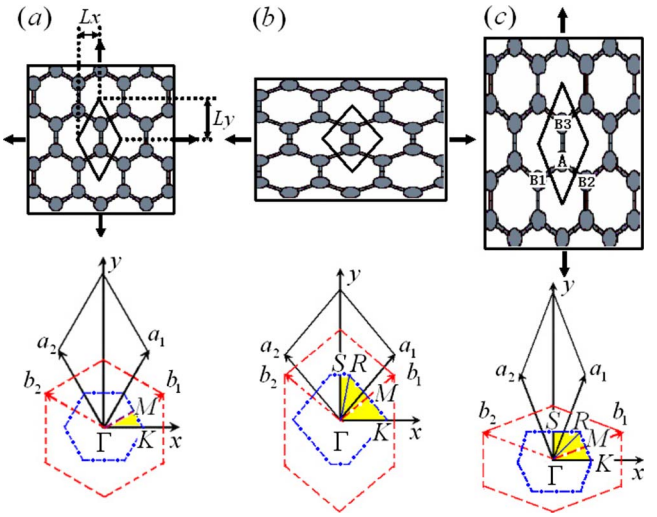

FIG. 1. (Color online) (a) Graphene system with symmetrical strain distribution, (b) asymmetrical strain distribution perpendicular to C-C bonds, and (c) asymmetrical strain distribution parallel to C-C bonds. Corresponding primitive cells (in black), reciprocal lattices (in red dashed), Brillouin zones [in blue (grey)], and irreducible Brillouin zones [in yellow (light grey)] are illustrated below the deformed lattices. Γ, *K*, *M*, *R*, and *S* are the high symmetrical points. L_x and L_y are the half diagonal lengths of the primitive cells.

broadens gradually as the lattice constant increases. At the lattice constant of 0.3759 nm, the high ELF splits into two equal parts. As the lattice constant reaches 0.4509 nm, one can only see large values of the ELF around each carbon atom, indicating that the C-C bond weakens gradually as increasing the lattice constant and eventually breaks down.

Figure 2(a) also shows that when the lattice constant is less than 0.3209 nm, band crossing occurs at the *K* point of the conduction and valence π bands. There is no band gap near the Fermi level. However, as the lattice constant is larger than 0.3209 nm, the shape of the band structure changes greatly and the DOS at the Fermi level is larger than zero, indicating that the system becomes metallic. From Fig. 2(a), we find that there exist two DOS peaks around the Fermi level, which form a pseudogap for the graphene system with a lattice constant less than 0.3209 nm. Figure 2(b) shows that the width of the pseudogap linearly decreases as the lattice constant increases.

It is well known that in graphene the sp^2 hybridization of the $2s$, $2p_x$, and $2p_y$ orbitals of carbon atoms create lateral σ bonds, and the remaining $2p_z$ orbitals form the π bands. Our detailed calculations show that the states near the Fermi level of the graphene systems with lattice constants varying from 0.2009 to 0.3159 nm are still determined by the $2p_z$ orbitals. Thus, we can use the TB approximation of the π orbitals to explain the change of the pseudogap as the lattice constant changes.

In the framework of the TB approximation, the energy dispersion[12] of a graphene system with lattice constant α is described by

$$E^{\pm}(\vec{k}) = \varepsilon_{2p} \mp \gamma f(\vec{k}), \tag{1}$$

with $f(\vec{k}) = \sqrt{1+4\cos\frac{\sqrt{3}k_x a}{2}\cos\frac{k_y a}{2}+4\cos^2\frac{k_x a}{2}}$ and $\gamma = \langle\varphi_A(\vec{r}-\vec{R}_A)|H|\varphi_B(\vec{r}-\vec{R}_A-\vec{R}_{1,i})\rangle$ $(i=1,2,3)$. Here, γ is the hopping

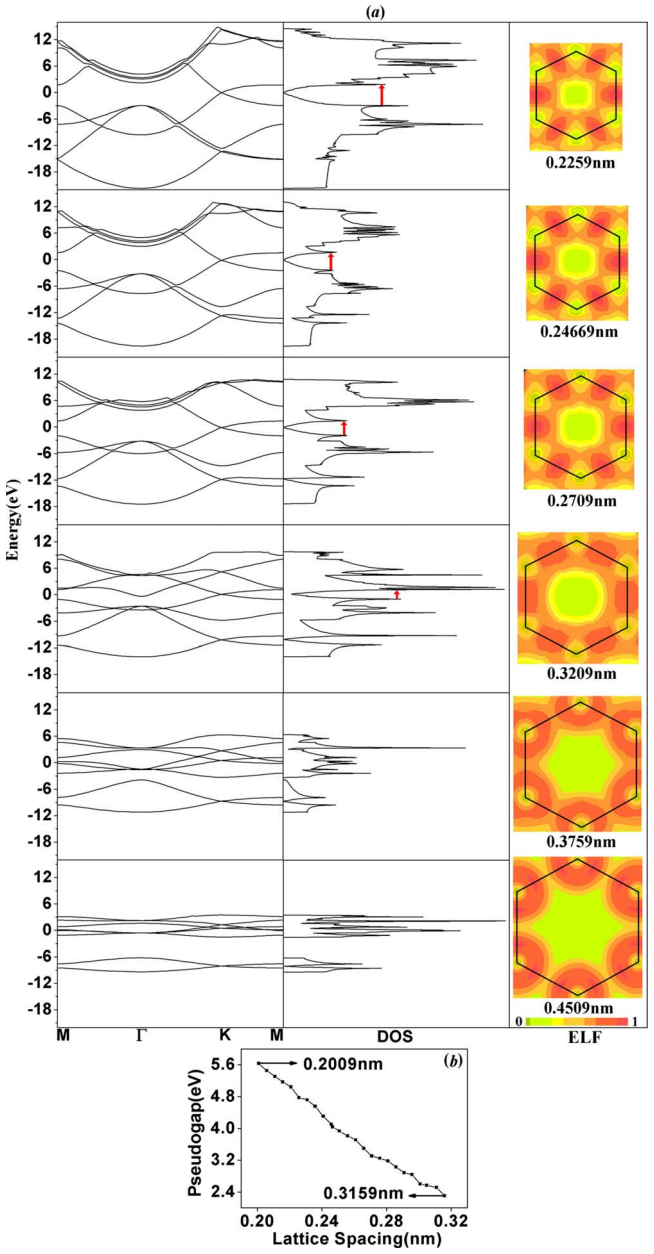

FIG. 2. (Color online) (a) The band structure, DOS, and ELF for symmetrical graphene systems with different values of lattice constant. (b) The pseudogap width (arrow) as a function of lattice constant.

integral, ε_{2p} is the energy of the C-$2p_z$ orbitals (a constant), and φ_A and φ_B are the C-$2p_z$ orbitals of the two *C* atoms at positions $\vec{R}_A$ and $\vec{R}_B$ in the primitive cell as shown in Fig. 1. The band-gap width is given by

$$E_{\text{gap}} = 2|\gamma|f(\vec{k}). \tag{2}$$

Because $f(\vec{k})$ is always zero at the *K* point of the Brillouin zone, the band-gap width keeps zero at the Fermi level for any values of the lattice constant. We found that the pseudogap is determined by the *M* point in the band structure where $f(\vec{k})=1$. As a result, the pseudogap width is given by $\Delta_{\text{pseudogap}}=2|\gamma|$, namely, linearly dependent on the hopping

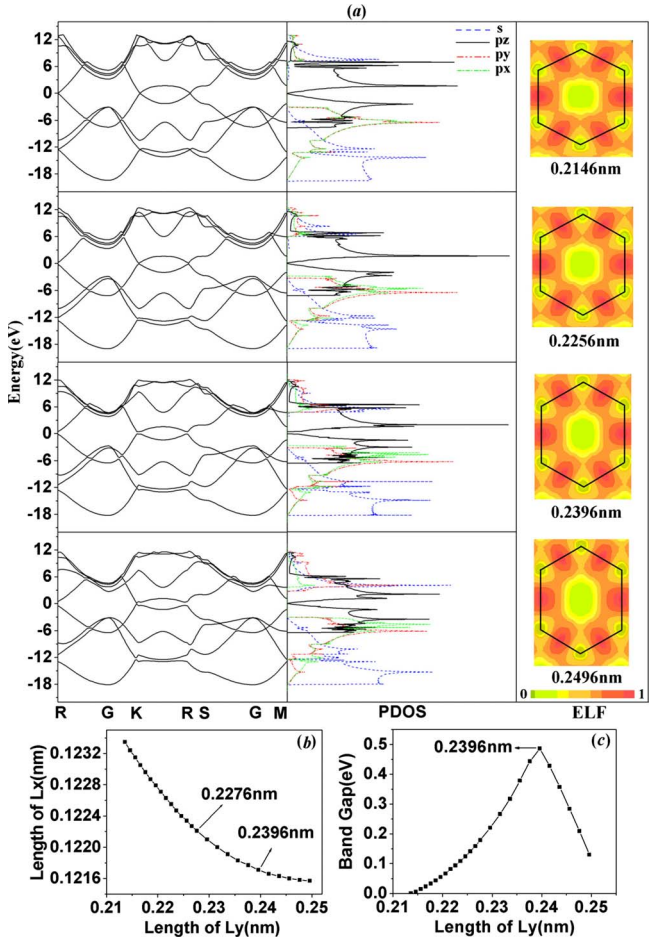

FIG. 3. (Color online) (a) The band structure, PDOS, and ELF for the graphene systems with asymmetrical strain distributions parallel to C-C bonds. (b) L_x as a function of L_y. (c) The band-gap width as a function of L_y.

integral γ. In general, a large lattice constant leads to a small value of $|\gamma|$. Therefore, our first-principles result is in agreement with the prediction by the above TB approach. Assuming that γ is linearly dependent on the lattice constant with $\gamma=A+B(a-a_0)$, we found $A=-2.094$ eV and $B=14.578$ eV/nm by fitting γ to the first-principles result in Fig. 2(b).

Asymmetrical strain distributions in graphene result in different results. To study the graphene system with asymmetrical strain distribution parallel to C-C bonds, we used a deformed primitive cell with a fixed value of L_y. The value of L_x was obtained as the system reaches its lowest total energy during structural relaxation. The deformed primitive cell with the given parameter L_y and the optimal parameter L_x was then used to calculate the electronic structure. The graphene systems with L_y varying from 0.2146 to 0.2496 nm were studied. Figure 3(a) shows the band structure, projected density of states (PDOS), and ELF of the asymmetrically deformed graphene systems with $L_y=0.2146$, 0.2256, 0.2396, and 0.2496 nm. The changes of L_x and the band-gap width are illustrated in Figs. 3(b) and 3(c), respectively. Figure 3(b) shows that L_x is linearly dependent on L_y as L_y is between 0.2136 (without deformation) and 0.2296 nm, indicating that the deformation is elastic. When L_y is larger than 0.2296 nm, L_x continues to decrease with a nonlinear decay behavior. A remarkable difference of the band structure for a graphene system with an asymmetrical strain distribution is that the symmetry breaking results in band-gap opening at the Fermi level. Figure 3(c) shows that the width of the band gap increases with L_y in the regime of $L_y<0.2396$ nm and then decreases for $L_y>0.2396$ nm. For $0.2136\ \text{nm}<L_y<0.2396$ nm, both the valence-band maximum and the conduction-band minimum locate at K and R points, indicating that the system has a direct band gap. For $L_y=0.2396$ nm, the conduction-band minimum locates at K point and the valence-band maximum locates at the left side of K point, indicating that the band gap is indirect. For $0.2396\ \text{nm}<L_y\leq 0.2496$ nm, both the valence-band maximum and the conduction-band minimum locate at the left side of K point and the band gaps become direct again.

The ELFs in Fig. 3(a) show that the shape of the high ELF regions elongates along the direction of L_y while being kept almost unchanged along the L_x direction. This indicates that the C-C bonds become weaker along the L_y direction while remaining strong along the L_x direction.

The PDOS in Fig. 3(a) shows that the states near the Fermi level are contributed mainly by the $2p_z$ orbitals. Thus, the π-orbital TB approximation is applicable to the system. We found that the energy dispersion of a graphene system with the above asymmetrical strain distribution is given by

$$E^{\pm}(\vec{k}) = \varepsilon_{2p} \mp |\omega|, \tag{3}$$

with

$$\omega = \gamma_1[e^{i\vec{k}\cdot\vec{R}_1} + e^{i\vec{k}\cdot\vec{R}_2}] + \gamma_2 e^{i\vec{k}\cdot\vec{R}_3},$$

$$\vec{R}_i = \vec{R}_{Bi} - \vec{R}_A \qquad (i=1,2,3),$$

$$\gamma_1 = \langle\varphi_A(\vec{r}-\vec{R}_A)|H|\varphi_B(\vec{r}-\vec{R}_{Bi})\rangle \qquad (i=1,2),$$

$$\gamma_2 = \langle\varphi_A(\vec{r}-\vec{R}_A)|H|\varphi_B(\vec{r}-\vec{R}_{B3})\rangle.$$

Here $\vec{R}_A$ and $\vec{R}_{Bi}$ are the positions of C atoms marked in Fig. 1(c). Equation (3) gives the band gap,

$$E_{\text{gap}} = 2|\omega|. \tag{4}$$

Because of the symmetry breaking, the hopping integral γ_1 is not equal to hopping integral γ_2. Our analysis to the function ω shows that the band gap can have nonzero values if γ_1 is not equal to γ_2. We found that the first-principles result of the band-gap width can be nicely given by Eq. (4) after choosing appropriate values of γ_1 and γ_2. Figure 4 shows the band structures of the graphene system with $L_y=0.2296$ nm calculated by the first-principles method (curves), and by Eq. (4) (symbols) using $\gamma_1=-2.491$ eV and $\gamma_2=-2.03$ eV. Apparently, two different methods give almost the same result in the energy region close to the Fermi level, showing the existence of a band gap of 0.22 eV. This confirms that it is the symmetry breaking that opens band gap at the Fermi level.

Similar behavior exists in the graphene system with asym-

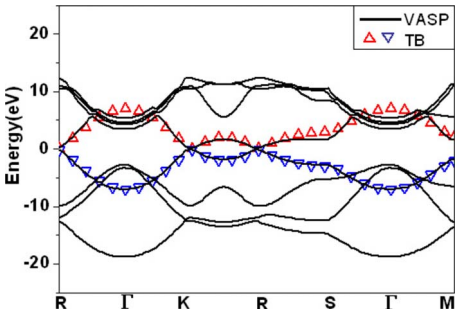

FIG. 4. (Color online) Band structures of the asymmetrical graphene system with L_y=0.2296 nm calculated by the first-principles method (curves) and the tight-binding method (symbols).

metrical strain distribution perpendicular to C-C bonds. In these systems, L_x was given by a value between 0.1243 and 0.1353 nm, and the value of L_y was obtained when the system reaches its lowest total energy during the structural optimization. The band structure, PDOS, and ELF for the systems with L_x of 0.1283, 0.1303, 0.1323, and 0.1343 nm are shown in Fig. 5(a). Changes of L_y and band gaps induced by different values of L_x are illustrated in Figs. 5(b) and 5(c), respectively. Figure 5(b) shows that the response of L_y is

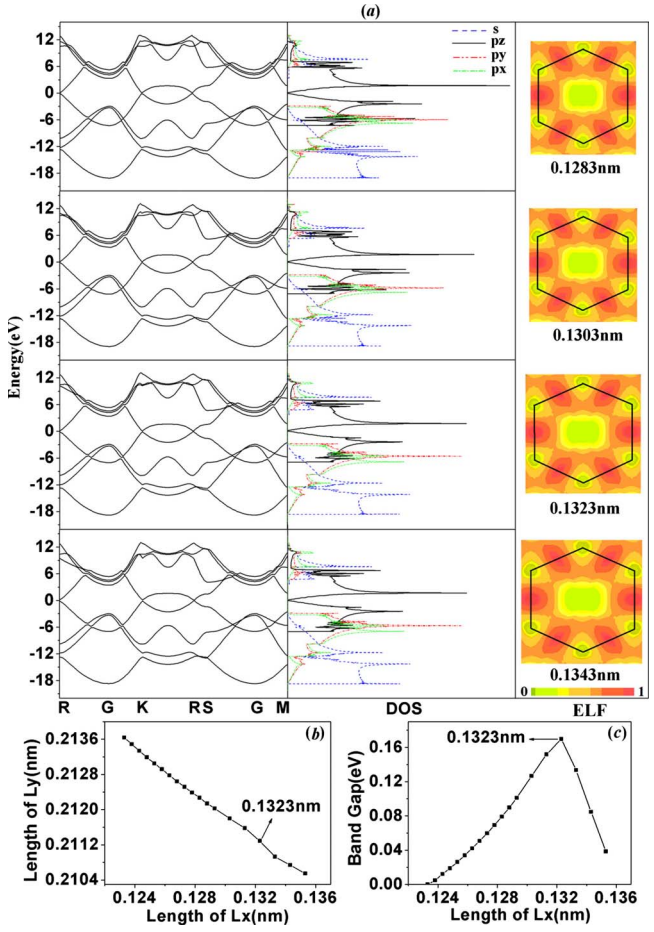

FIG. 5. (Color online) (a) The band structure, PDOS, and ELF for the graphene systems with asymmetrical strain distributions perpendicular to C-C bonds. (b) L_y as a function of L_x. (c) The band-gap width as a function of L_x.

linear and thus elastic in the range of 0.1233 nm$<L_x<$0.1323 nm, where 0.1233 corresponds to the standard graphene without deformation. For $L_x>0.1323$ nm, L_y continues to decrease but deviates from the linear behavior. Figure 5(c) shows that in the elastic region with $L_x<0.1323$ nm, the band-gap width increases as L_x increases, whereas it decreases in the nonelastic region with $L_x>0.1323$ nm. For 0.1233 nm$<L_x<$0.1323 nm, both the valence-band maximum and the conduction-band minimum locate at K and R points, indicating that the system has a direct band gap. For L_x=0.1323 nm, the conduction-band minimum locates at R point and the valence-band maximum locates at the right side of R point, indicating that the band gap is indirect. When L_x is in the nonelastic region, both the valence-band maximum and the conduction-band minimum locate at the right side of R point, and thus the band gap becomes direct again.

The PDOS in Fig. 5(a) shows that the states around the Fermi level are mainly contributed by the $2p_z$ orbitals of carbon atoms. Using the same TB approach as described in Eq. (3), we found that the band-gap width obtained by the first-principles method can be nicely reproduced by the TB model as well. This further confirms that symmetry breaking in graphene leads to band-gap opening at the Fermi level.

In summary, the electronic properties of graphene systems with different types of strain distributions have been studied by the *ab initio* calculations and the TB approach. Our results show that the nature of the band structure of graphene depends on its lattice symmetry. With a symmetrical strain distribution, the graphene does not open a band gap at the Fermi level. In this case, one finds zero density of states at the Fermi level and its pseudogap decreases linearly as the strain increases. Asymmetrical strain distributions in graphene open band gaps at the Fermi level. For the strain distribution parallel to C-C bonds, the band gap increases from 0 to 0.486 eV as the strain increases to 13.1% before it decreases under large deformation. For the strain distribution perpendicular to C-C bonds, the band gap increases from 0 to 0.170 eV as the strain increases to 4.91% before decreasing. Clearly, the strain distribution parallel to C-C bonds induces larger band gaps compared with the strain distribution perpendicular to C-C bonds.

We found that the anisotropic nature of the band-gap opening of graphene under large strain is reflected by different Poisson ratios in different directions. Figure 6 illustrates the Poisson ratios ν_x and ν_y in the directions perpendicular to or parallel to C-C bonds; here the Poisson ratios were calculated directly using the definitions $\nu_x=(\Delta L_x/L_x)/(\Delta L_y/L_y)$ and $\nu_y=(\Delta L_y/L_y)/(\Delta L_x/L_x)$. Figure 6 shows that, under small strain (less than 2%), the Poisson ratios in the two directions take the same values, indicating that graphene is isotropic under small strain. Under even smaller strain less than 1.5%, we found that the Poisson ratios are a constant of 0.1732. However, in the regime of large strain (larger than 2%), the two Poisson ratios apparently follow two different decay behaviors, indicating that graphene is anisotropic under large deformation. We note that understanding the elastic properties of 2D graphene is not trivial due to the many-body interatomic interactions as well as the charge redistributions under finite deformations. Early studies suggested that the

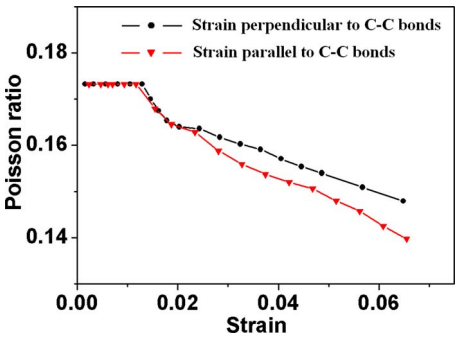

FIG. 6. (Color online) Poisson ratios of graphene under strains parallel to or perpendicular to C-C bonds.

2D hexagonal symmetry of pure *C* lattice ensure its isotropic elastic properties and thus can be described by an isotropic shell model.[18–20] The isotropic Poisson ratio under small deformations was found to be 0.149 by first-principles calculations,[20] which is close to the constant value of 0.1732 we obtained under small strain. Recently, a finite deformation continuum theory was derived from classical interatomic potentials for the analysis of the elastic properties of 2D graphene and carbon nanotubes,[21] which shows that only the infinitesimal elasticity tensor of 2D honeycomb lattices is isotropic, leading to a Poisson ratio of 0.412 on the basis of Brenner's potential. The theory also pointed out that the elastic properties of graphene under finite deformations can be anisotropic. Molecular-dynamics simulations based on Brenner's potential were performed for understanding the elastic properties of finite graphene sheets with finite deformation and the computed elastic constants of rectangular-shaped graphene sheets were found to conform to orthotropic material behavior.[22] For the rectangular graphene sheet with only two edges constrained to be straight, the Poisson ratio is 0.416 and 0.465 for the strain distribution parallel to or perpendicular to C-C bonds, respectively. For the rectangular graphene sheet with four edges constrained to be straight, the Poisson ratio is 0.428 and 0.520 for the strain distribution parallel to or perpendicular to C-C bonds, respectively. Our first-principles result about the anisotropic behavior of the Poisson ratio for the graphene under large strain qualitatively agrees well with the trend observed in the molecular-dynamics study. We note that, because large strains induce significant changes of the band-gap structure and electron redistribution, the elasticity anisotropy of graphene is a quantum effect that cannot be elucidated completely by applying the classical theory of elasticity. This is why classical potentials can only give a Poisson ratio that is almost three times larger than the values obtained by the first-principles calculations.

In general, breaking the hexagonal symmetry is expected to modify the band structure of graphene.[9,10] In previous studies, the symmetry breaking of graphene is introduced either by substrates or by cutting graphene to form ribbons. It has been demonstrated that the asymmetrical surface of SiC induced by the surface reconstruction opens band gaps in graphene.[9] It has also been shown that breaking the symmetry of graphene by cutting it along different directions leads to graphene ribbons with very different electronic properties.[23–25] The ribbons with zigzag edges obtained by cutting graphene along the direction perpendicular to C-C bonds are metals while those with armchair edges obtained by cutting graphene along the direction parallel to C-C bonds are semiconductors.[23–25] In our situation, symmetry breaking is induced by the strain perpendicular or parallel to C-C bonds, which corresponds to the zigzag edge or the armchair directions, respectively. Therefore, our results about the anisotropic behaviors of the band structure and the Poisson ratio are in agreement with existing findings in graphene. The anisotropy can be understood by considering the consequences under large strains. The large strain parallel to C-C bonds leads to weakly coupled zigzag carbon chains while the large strain perpendicular to C-C chains results in weakly coupled carbon dimmers. It is understandable that the two different structures have different elastic properties. We note that despite the interest of graphite as basic building block for a variety of nanostructured materials, there is no complete and reliable data set of its elastic properties. The experimental difficulty comes from the lack of large single crystals while the computational efforts are limited by the two completely different types of interatomic bonding—exceptionally strong intralayer bonding and the weak van der Waals interlayer bonding. Experiments using pyrolytic graphite[26] only observed the significant difference between the in-plane Poisson ratio (ν=0.16) and the out-of-plane Poisson ratio (ν=0.012) but failed in revealing the in-plane anisotropy due to the large amount of randomly oriented crystallites in the samples. Confirmation of the anisotropic nature of graphene requires further experimental studies using high-quality samples of crystalline graphene and graphite.

It was recently proposed that spin-orbital coupling in graphene also leads to gap opening.[5–8] However, first-principles calculations[8] showed that the gap induced by the spin-orbital coupling is very small: about 10^{-6} eV. Our study indicates that the band gap of graphene can be tuned in the order of 10^{-1} eV not only by the strength but also by the direction of the strain. Evidently, the strain distributions dominate the gap opening in graphene. Our findings are important for understanding and controlling the transport properties of graphene systems.

This work was supported by the Chang Jiang Scholars Program, Ministry of Education, China, and by the National Natural Science Foundation of China (Grant No. 10774127).

*Corresponding author.jxzhong@xtu.edu.cn

[1] K. S. Novoselov, A. K. Geim, S. V. Morozov, D. Jiang, Y. Zhang, S. V. Dubonos, I. V. Grigorieva, and A. A. Firsov, Science **306**, 666 (2004).
[2] K. S. Novoselov, D. Jiang, F. Schedin, T. J. Booth, V. V. Khotkevich, S. V. Morozov, and A. K. Geim, Proc. Natl. Acad. Sci. U.S.A. **102**, 10451 (2005).
[3] K. S. Novoselov, A. K. Geim, S. V. Morozov, D. Jiang, M. I. Katsnelson, I. V. Grigorieva, S. V. Dubonos, and A. A. Firsov, Nature (London) **438**, 197 (2005).
[4] Y. B. Zhang, Y. W. Tan, H. L. Stormer, and Ph. Kim, Nature (London) **438**, 201 (2005).
[5] C. L. Kane and E. J. Mele, Phys. Rev. Lett. **95**, 226801 (2005).
[6] D. Huertas-Hernando, F. Guinea, and A. Brataas, Phys. Rev. B **74**, 155426 (2006).
[7] H. Min, J. E. Hill, N. A. Sinitsyn, B. R. Sahu, L. Kleinman, and A. H. MacDonald, Phys. Rev. B **74**, 165310 (2006).
[8] Y. Yao, F. Ye, X. L. Qi, S. C. Zhang, and Z. Fang, Phys. Rev. B **75**, 041401(R) (2007).
[9] S. Y. Zhou, G. H. Gweon, A. V. Fedorov, P. First, W. de Heer, D.-H. Lee, F. Guinea, A. C. Neto, and A. Lanzara, Nat. Mater. **6**, 770 (2007).
[10] D. Xiao, W. Yao, and Q. Niu, Phys. Rev. Lett. **99**, 236809 (2007); W. Yao, D. Xiao, and Q. Niu, Phys. Rev. B **77**, 235406 (2008).
[11] G. Kresse and J. Furthmüller, Comput. Mater. Sci. **6**, 15 (1996).
[12] G. Kresse and J. Furthmüller, Phys. Rev. B **54**, 11169 (1996).
[13] P. E. Blöchl, Phys. Rev. B **50**, 17953 (1994).
[14] G. Kresse and D. Joubert, Phys. Rev. B **59**, 1758 (1999).
[15] J. P. Perdew and Y. Wang, Phys. Rev. B **45**, 13244 (1992).
[16] H. J. Monkhorst and J. D. Pack, Phys. Rev. B **13**, 5188 (1976).
[17] R. Saito, M. Fujita, G. Dresselhaus, and M. S. Dresselhaus, *Physical Properties of Carbon Nanotubes* (Imperial College London, London, 1998).
[18] J. Tersoff and R. S. Ruoff, Phys. Rev. Lett. **73**, 676 (1994).
[19] B. I. Yakobson, C. J. Brabec, and J. Bernholc, Phys. Rev. Lett. **76**, 2511 (1996).
[20] K. N. Kudin, G. E. Scuseria, and B. I. Yakobson, Phys. Rev. B **64**, 235406 (2001).
[21] M. Arroyo and T. Belytschko, Phys. Rev. B **69**, 115415 (2004).
[22] C. D. Reddy, S. Rajendran, and K. M. Liew, Nanotechnology **17**, 864 (2006).
[23] K. Nakada, M. Fujita, G. Dresselhaus, and M. S. Dresselhaus, Phys. Rev. B **54**, 17954 (1996).
[24] Y. W. Son, M. L. Cohen, and S. G. Louie, Phys. Rev. Lett. **97**, 216803 (2006).
[25] Y. W. Son, M. L. Cohen, and S. G. Louie, Nature (London) **444**, 347 (2006).
[26] O. L. Blakslee, D. G. Proctor, E. J. Seldin, G. B. Spence, and T. Weng, J. Appl. Phys. **41**, 3373 (1970); E. J. Seldin and C. W. Nezbeda, *ibid.* **41**, 3389 (1970); J. P. Lu, Phys. Rev. Lett. **79**, 1297 (1997).